Phase Behavior and Thermodynamics of a Mixture of Cationic Gemini and Anionic Surfactant

Yujie Wang,[†] Guangyue Bai,[†,‡] Eduardo F. Marques,*[,†] and Haike Yan*[,‡]

Centro de Investigação em Química, Department of Chemistry, Faculty of Sciences, University of Porto, Rua do Campo Alegre, no. 687, P-4169-007 Porto, Portugal, and Center of Molecular Science, Institute of Chemistry, Chinese Academy of Sciences, Beijing, 100080, P. R. China

Received: August 4, 2005; In Final Form: November 28, 2005

We present the phase behavior and thermodynamics of the catanionic mixture of the gemini surfactant hexanediyl-α,ω-bis(dodecyldimethylammonium bromide), designated here as 12-6-12Br_2, and sodium dodecyl sulfate (SDS) over the full range of composition, at the water-rich corner. Visual and turbidity measurements of the mixtures provide some basic macroscopic information on phase behavior. The structure of the aggregates formed spontaneously in the mixtures has been observed with TEM. As the molar fraction of SDS, X_{SDS}, is increased, at constant total surfactant concentration, the aggregation morphologies change gradually from gemini-rich micelles, through multiphase regions containing a precipitate (catanionic surfactant) and a vesicle region, to SDS-rich micelles. From isothermal titration calorimetry measurements, the phase boundaries and corresponding enthalpy changes for phase transitions have been obtained. The formation of the different microstructures, in particular, the spontaneously formed vesicles in the SDS-rich side, is discussed on the basis of geometric and electrostatic effects occurring in the SDS−gemini mixture.

1. Introduction

In recent years, studies on gemini surfactants have attracted increasing attention because of their many unusual physicochemical properties in comparison with those of conventional surfactants.[1−5] One of the most striking features of alkanediyl-α,ω-bis(dodecyldimethylammonium bromides), a series of cationic gemini surfactants, designated here as 12-*s*-12Br_2 with $s = 2, 3, 4, 5$, and so forth, is their unusual and wide range of self-assembled morphologies in aqueous solutions.[3d,6−8] Cryo-transmission electron microscopy (cryo-TEM) has clearly shown that the aggregation morphologies of the 12-*s*-12Br_2 series in aqueous solution are controlled by the length of the spacer groups.[6a,d] Gemini surfactants with short spacers ($s = 2$ or 3) always form entangled, threadlike or wormlike micelles even at low concentrations, i.e., aggregates of lower curvature, whereas the corresponding monomeric surfactant DTAB (dodecyltrimethylammonium bromide) forms only spheroidal micelles. Zana et al.[2,6a,d] have shown that the 12-*s*-12Br_2 surfactants have a sequence of morphologies from elongated micelles through spherical micelles to vesicles as *s* increases.

Since mixtures of different surfactants often form new types of aggregates or show a growth of aggregates in one or more dimensions, there have been a number of studies on their phase behavior and microstructure, especially for catanionic mixtures. The most commonly studied catanionic mixtures have been those containing anionic sodium alkyl sulfates and cationic alkylammonium halides.[9−11] In contrast, there have been few reports on the aggregation behavior of mixtures of cationic gemini and other surfactants. Alargova et al. have studied the critical micelle concentration (cmc) effects of mixing cationic geminis with single-chain cationic and nonionic surfactants.[12] Talmon et al. have examined the change in microstructure when a cationic gemini with a short spacer is added progressively to a vesicle forming cationic gemini with a large spacer.[13] Battacharya et al. have studied the formation of vesicles from the ion-paired amphiphiles, bis(hexadecyldimethylammonium)-alkane dipalmitate, by means of reverse-phase evaporation or direct mixing.[14] Cationic gemini surfactants having nucleotides as counterions show transitions to hydrogels upon addition of complementary nucleoside bases or other nucleo-gemini surfactants having complementary bases as counterions.[15] Oda and Bourdieu[16] have reported a micelle−vesicle transition induced by the addition of a neutral cosurfactant, hexanol, into a wormlike micellar solution of 12-2-12Br_2. The morphology of the mixtures exhibited features characteristic of wormlike micelles, elongated ribbons, and multilayered phases, depending on the concentration and composition. Mixtures of cationic gemini with its corresponding monomeric surfactant form only mixed micelles.[17,18]

In this work, we focus on the solution microstructure and the interaction thermodynamics of the gemini 12-6-12Br_2 with the most common anionic surfactant, SDS. The nearest system to this catanionic mixture is the mixture of cationic geminis with methyl orange, where aggregation into a number of structures, including vesicles, has been observed by Buwalda.[19] The much wider range of aggregate structures exhibited by the mixed system as compared to the single-surfactant solutions is the complex result of the intermolecular and interaggregate interactions. A first natural step in the study of the mixtures is the building of phase diagrams, where single-phase and multiphase regions are depicted. The direct imaging of the samples by microscopy techniques (electron or light microscopy) is also crucial for the determination of the microstructures present in solution phases. Some interactions are not present in single-surfactant solutions, even for covalent zwitterionic surfactants.[20]

* Corresponding authors. Eduardo F. Marques: efmarque@fc.up.pt; fax +351 226082959; tel. +351 226082835. Haike Yan: hkyan@iccas.ac.cn.
† University of Porto.
‡ Chinese Academy of Sciences.

10.1021/jp054323z CCC: $33.50
Published on Web 02/23/2006

So, any understanding of the mechanism of formation of mixed-surfactant aggregates should also be based partly on the thermodynamics of the process, and for this purpose, the interaction energy that can be measured directly by isothermal titration microcalorimetry (ITC) is one of the most important parameters. Furthermore, this technique can be very useful in the determination of boundaries between two-phase regions.[21]

2. Experimental Section

2.1. Materials. The gemini surfactant hexanediyl-α,ω-bis-(dodecyldimethylammonium bromide), was synthesized and purified according to the method of Menger.[1] The following materials were used for the synthesis, without further purification: 1,6-dibromohexane (96%, Aldrich) and 1-dimethylaminododecane (≥97%, Fluka). The good purity of the product was checked and confirmed by NMR, elemental analysis, and surface tension. SDS (≥97%) was purchased from Sigma and used as received, revealing a small well on the surface tension vs log *c* plot and a cmc of ca. 8 mM.

2.2. Sample Preparation and Phase Behavior. The mixed samples of 12-6-12Br_2 and SDS (1 mL) were prepared by volume from 1 wt % stock solutions of the single surfactants 12-6-12Br_2 and SDS. The total concentration of the mixtures was 1 wt %, and the equilibrated samples were diluted to other sample series with identical mixing ratio and lower total surfactant concentration. The composition of the samples is also expressed as the molar fraction of SDS, defined as $X_{SDS} = n_{SDS}/(n_{SDS} + n_{12-6-12Br_2})$, for comparison with isothermal titration calorimetry. The samples were heated and cooled repeatedly between room temperature and 50 °C several times and then kept at room temperature for about 1 year. The phase behavior of the mixtures was initially inspected by visual observations.

2.3. UV−vis Spectroscopy. The turbidity of the mixed solutions was measured on a General TU-1201 UV−vis spectrophotometer in 1-cm-thick quartz sample cells. The concentrations of the surfactant solutions were the same as those for the TEM experiments (see below), and the solutions were about 1 year old.

2.4. Transmission Electron Microscopy (TEM). Sample imaging was carried out by TEM, by means of a Hitachi H800 microscope, using the negative staining method.[11] The total surfactant concentration of all the samples was 2 mM, and the mole fraction of SDS, X_{SDS}, was varied from 0 to 0.95 with an increment of 0.05. The samples for TEM observation were made by deposition of solution on the grid, drying in a desiccator, and staining with 1.5 wt % of uranyl acetate solution. Although the sign of the surface charge of the mixed surfactant aggregates may be positive or negative, depending on the ratio of cationic and anionic surfactants, Lukac et al. have demonstrated by the standard drop method that there are no artifacts of the staining procedure on the aggregation features.[22]

2.5. Isothermal Titration Calorimetry (ITC). The calorimeter used in this work was an improved LKB-2107 isothermal titration microcalorimeter with a 1 mL sample cell. The experimental procedure has been described in detail in previous works by us.[5,11] Briefly, this instrument has an electrical calibration with precision better than 1%. Its accuracy was checked by measuring the dilution enthalpy of a concentrated sucrose solution according to the method described elsewhere.[23] Concentrated SDS solution was injected in small aliquots into the stirred sample cell with pure water or gemini surfactant solution using a 250 or 500 μL Hamilton syringe controlled by a Braun 871182 pump. Each aliquot was 4−10 μL, and addition of concentrated solution continued until the desired range of concentration had been covered. The interval between two injections was kept sufficiently long so that the signal could return to the baseline. The observed enthalpy was obtained by integration over the peak in voltage (*V*)−time (*t*) plot. All experiments were performed at 303.15 ± 0.02 K and were repeated at least three times.

2.5. Conductivity Measurements. The electrical conductivity of single- and mixed-surfactant solutions was measured with a CDM210 conductivity meter (CDC641T electrode, France) in a double-walled vessel with flowing thermostated water at 30 °C. The conductimeter was initially calibrated with standard solutions of known conductivity (KCl, 0.01 and 0.1 M).

2.6. Surface Pressure Measurements. For the surface pressure measurements, a Langmuir trough (KSV Instruments Ltd., Helsinki) controlled by computer with 364 mm length and 75 mm width was used. The trough was thermostated at 20.0 ± 0.1 °C by a Julabo F12-MV bath. A surfactant solution with mixed chloroform−methanol 95/5 (v/v) as solvent was spread onto the subphase with a SGE gastight syringe. After 30 min for solvent evaporation, the isotherm was recorded with a constant compression rate of 5 mm min^{-1}.

3. Results and Discussion

3.1. Phase Behavior from Visual Observations and Turbidity. The mixed gemini−SDS samples were visually observed in the course of several months in order to ascertain equilibration and to look for the different macroscopic phases present. The samples were also looked at between crossed polaroids in order to check for birefringence. An important point to be noted is that for a system composed of a cationic surfactant A^+X^-, an anionic surfactant A^-X^+, and water, with no common ion, there are four components in observance of the Gibbs phase rule.[9e] This stems from (i) the possibility of having the salts A^+A^- (catanionic surfactant) and X^+X^- (simple electrolyte) in addition to the cationic and anionic surfactant salts and (ii) the electroneutrality principle. Nonetheless, catanionic mixtures have been conveniently treated as quasi-ternary systems, as supported by experimental evidence.[9,10] Thus, ternary phase diagrams are commonly used, where not only single-phase regions but also the experimentally observed heterogeneous regions are depicted. The same approach is followed here, bearing in mind also that our main focus is the single-phase regions.

The total surfactant concentration is 1 wt % for the samples henceforth described, and the composition will be also given in X_{SDS}. In the binary systems SDS−water and 12-6-12−water, up to the concentration range of 1 wt % investigated in this work, spheroidal micelle solutions[2] are found, with cmc values of 0.23 wt % (8.3 mM) for SDS and 0.066 wt % (0.99 mM) for the gemini. Therefore, there are two mixed-micelle solution regions both in the 12-6-12Br_2-rich and SDS-rich sides, but the boundaries cannot be clearly defined just by visual observations. Starting from the gemini−water axis, the aqueous mixtures in the range 1−0.99 wt % 12-6-12Br_2 (X_{SDS} = 0−0.03) form a colorless solution. For the range 0.98−0.65 wt % 12-6-12Br_2, (X_{SDS} = 0.04−0.56), they exhibit two phases, a colorless solution and a solid precipitate at the bottom. For the range 0.64−0.55 12-6-12Br_2 wt % (X_{SDS} = 0.57−0.66), there is a precipitate, a middle turbid solution phase, and another phase with lower density floating at the surface of the liquid phase, so that the system yields here a three-phase region. The nature of the upper phase is not totally clear, but it can be described as a waxy material, either an amorphous solid or, more likely, a liquid-crystalline phase. It should be emphasized that the macroscopic phases are stable for more than 1 year and do not

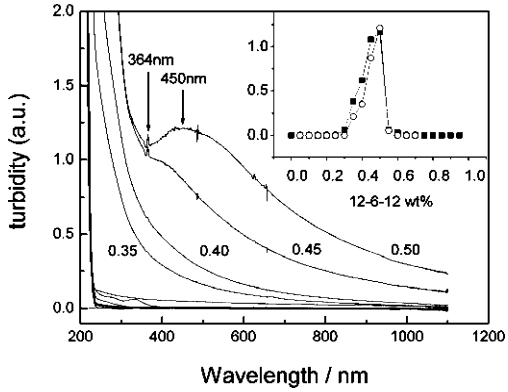

Figure 1. Turbidity of the mixtures of 12-6-12Br_2 and SDS with a constant total concentration of 1 wt %, at 30 °C. The inset is the turbidity as a function of the wt % of 12-6-12Br_2, at 450 nm (○) and 364 nm (●).

change with the total surfactant concentration in the studied range. Samples in the very narrow range 0.54−0.50 wt % gemini (X_{SDS} = 0.66−0.70) contain a precipitate and a clear solution. For the range 0.49−0.46 wt % gemini (X_{SDS} = 0.71−0.73), the precipitate is in equilibrium with a bluish solution, whereas below 0.45 gemini wt % (X_{SDS} > 0.74), the precipitate is totally redissolved, and only a one-phase solution region exists. This solution is bluish for 0.45−0.38 wt % gemini (X_{SDS} = 0.74−0.79), but it becomes colorless below ca. 0.34 wt % gemini (X_{SDS} > 0.82).

In Figure 1, the UV−vis absorbance spectra of 12-6-12/SDS samples, 1 year after preparation, are shown. Also shown, as an inset, is the change in turbidity measured at 450 and 364 nm as a function of X_{SDS}, at a total surfactant concentration of 1 wt %. As mentioned above, the liquid phases of the mixtures in the range 0.35−0.55 wt % gemini (approximately) appear as turbid bluish. Since there is no chromophore in either gemini or SDS molecules, it is the scattering from aggregates or particles which is responsible for the bluish appearance. Below 0.35 and above 0.55 wt % 12-6-12Br_2, the liquid phase of the samples does not exhibit any absorption band (Figure 1), while in the range 0.35−0.50 wt %, a relatively strong broad band appears, with maximum intensity at around 450 nm, as can be seen for 0.50 wt %, which is related with the strong turbidity. This band appears first at 0.45 wt % gemini, and its intensity at 450 nm reaches a maximum value at the equicharged composition, 0.55 wt % gemini. At 436 nm, a peak corresponding to the bluish liquid phase appears, also given in the inset. The turbidity then decreases gradually as the concentration of gemini decreases until 0.35 wt % (Figure 1, inset). The boundary between the bluish and colorless phases appears thus at about 0.34−0.35 wt % gemini.

3.2. Aggregate Structure in the Liquid Phases: TEM Observations. To determine the aggregate structure for the bluish and colorless liquid phases observed in this catanionic mixture, TEM observations were carried out for six-month-aged samples. The upper liquid phase for two-phase samples and the middle liquid phase of the three-phase samples were inspected. Also, bluish and colorless one-phase samples were observed. Figure 2a shows a representative micrograph for the upper bluish solution in equilibrium with a precipitate, at ca. 0.49 wt % gemini (X_{SDS} = 0.70). Figure 2b shows another representative micrograph for a sample in the bluish single-phase solution, at 0.44 wt % gemini (X_{SDS} = 0.75). In both cases, it is possible to see the presence of vesicle aggregates. Even though the aggregate size cannot be determined accurately with the method used, it is possible to state that the vesicles range in size approximately between 50 and 400 nm. Near the equicharge line in the three-phase region side, no vesicle aggregates were found, indicating that the vesicles occur as single phase only for the excess SDS side. In the samples containing a colorless solution (<0.34 wt % gemini, X_{SDS} > 0.82), no vesicle agregates were found, but instead very small aggregates were observed, appearing as dot-like in the TEM micrographs and identified as micelles (not shown here).

3.3. Aggregation Thermodynamics and Phase Boundaries: ITC Measurements. In a catanionic mixture of the type of the gemini−SDS mixture, the changes in the aggregation state with surfactant mixing ratio are often gradual. These changes can be somewhat difficult to track experimentally. ITC is undoubtedly a technique that can be of great value for this purpose, besides yielding direct enthalpy values for the transitions. Figure 3a shows the interaction enthalpy as a function of SDS molar fraction, for four different initial concentrations of 12-6-12Br_2, 0.5, 2.0, 3.5, and 5.0 mM (which correspond in wt % to 0.34, 0.23, 0.13, and 0.034). Considering the first titration, as shown in Figure 3a, the observed enthalpies vary from −33.3 kJ mol^{-1} to −25.2 kJ mol^{-1} (Table 1, ΔH_{inter}), as the concentration of 12-6-12Br_2 increases from 0.5 mM to 5 mM, meaning that the exothermic effect decreases with increasing concentration of 12-6-12Br_2 in the cell. Note that the aggregation state of SDS in the syringe is the micelle, and the observed enthalpies are the resulting sum of the micellar dissociation (ΔH_{mic} = −5.2 kJ mol^{-1}, value from a previous work[24]) and the interaction between SDS and 12-6-12Br_2. But when we compare the interaction with different 12-6-12Br_2 concentrations, the contribution of SDS dissociation is practically identical

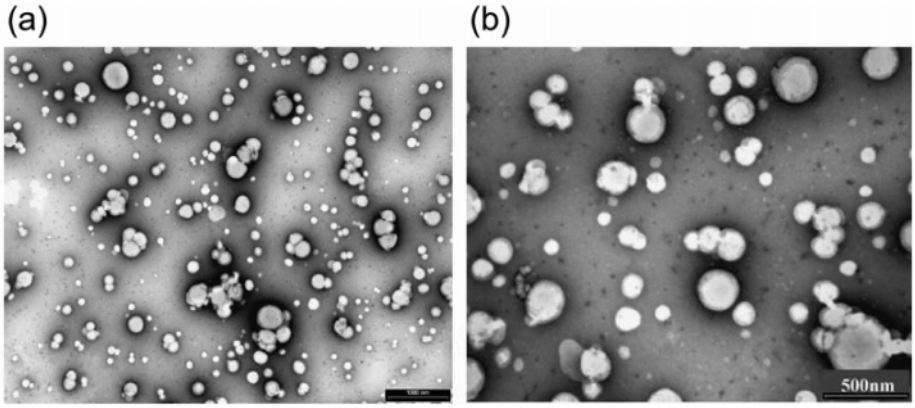

Figure 2. TEM images of the mixtures of 12-6-12Br_2 and SDS with a constant total concentration of 2 mM: (a) vesicle aggregates at 0.49 wt % gemini (X_{SDS} = 0.70), upper liquid phase of two-phase sample; (b) vesicle aggregates at 0.44 wt % gemini (X_{SDS} = 0.75), bluish solution phase.

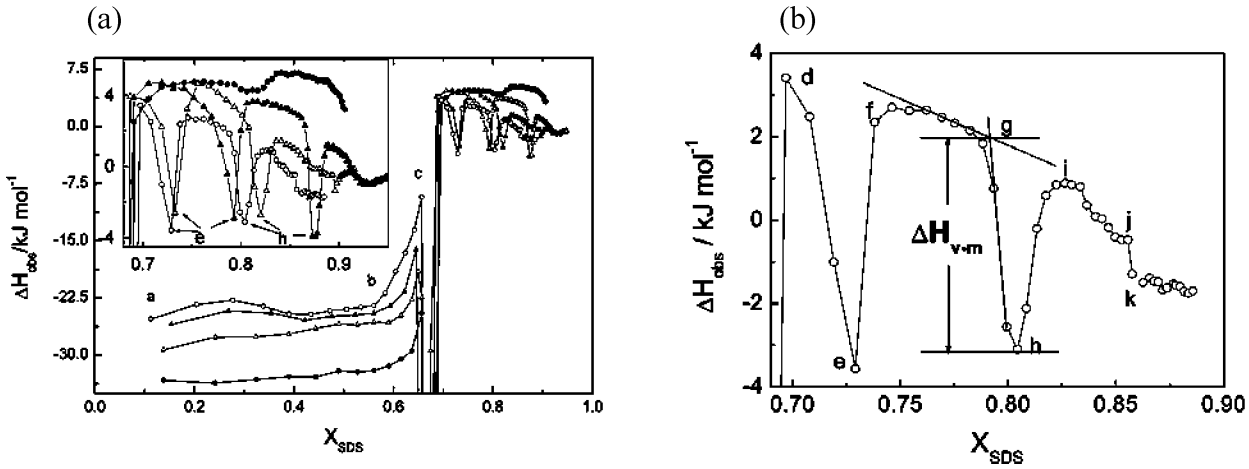

Figure 3. The observed enthalpy measured by ITC, at 30 °C, as a function of the molar fraction of SDS in the mixtures of SDS and 12-6-12Br_2: (a) at varying initial concentrations of 12-6-12Br_2, 0.5 mM (●), 2.0 mM (△), 3.5 mM (▲), and 5 mM (○); (b) expansion of region for $X_{SDS} > 0.65$, for the initial 5 mM 12-6-12Br_2 sample.

TABLE 1: Interaction Enthalpy and Enthalpy for Transition from Catanionic Surfactant to Vesicle and from Vesicle to Micelle with Their Corresponding Molar Fractions of SDS as Determined by ITC

$C_{12-6-12}$/mM	ΔH_{inter}/kJ mol^{-1}	X_{SDS}	ΔH_{CS-V}/kJ mol^{-1}	X_{SDS}	ΔH_{V-M}/kJ mol^{-1}
5.0	-25.2 ± 0.2	0.728	-7.0 ± 0.2	0.800	-7.2 ± 0.2
3.5	-26.0 ± 0.2	0.733	-6.5 ± 0.2	0.819	-7.2 ± 0.2
2.0	-29.2 ± 0.2	0.793	-5.5 ± 0.2	0.875	-6.5 ± 0.2
0.5	-33.3 ± 0.2	0.805 ± 0.817	-0.4 ± 0.2[a]		

[a] The catanionic surfactant may transform into micelles without the vesicle morphology for this concentration.

for all the systems. Thus, the variation of enthalpies is caused mainly by the effect of the aggregation state of 12-6-12Br_2 in the cell. Furthermore, since 12-6-12Br_2 and SDS have identical chain lengths, the hydrophobic interaction between the same molecules or the different molecules is approximately equal.

When the concentration of 12-6-12Br_2 is 0.5 mM, that is smaller than the surfactant cmc (0.99 mM), addition of SDS solution causes the mixed micelle to be formed. As the concentration of gemini increases in the cell, above the cmc, the observed exothermic enthalpies decrease. The change of the observed enthalpies should be related with the micellar morphology. The electrostatic screening of counterions on the micelle surface weakens the interaction between the oppositely charged headgroups of 12-6-12Br_2 and SDS. Thus, the observed exothermic enthalpies decrease, since the micellar concentration is higher at higher 12-6-12Br_2 concentrations. Moreover, the monomer concentration above the cmc decreases slightly with concentration, making the interaction somewhat less favorable.[25−31] These two factors are behind the decrease in exothermic enthalpy. Between a and b, in Figure 3a, the curve is seen as a broad peak which flattens out upon decreasing concentration of 12-6-12Br_2 and even disappears below the cmc.

Comparing Figure 3b and phase behavior observations decribed in section 3.1, the component from b to e can be divided into three regions: b−c, c−d, and d−e. The rise from b to c corresponds to the triphasic region where a solid, a turbid liquid, and another phase with lower density on the liquid surface are seen. In this region, it is difficult to determine the exact physical meaning of the observed enthalpy for the complex multiphasic behavior. Between c and d (second region), there is a very narrow exothermic peak with a peak top at exactly equicharge molar ratio, $X_{SDS} = 0.66$ (negative peak top not shown in Figure 3a). Therefore, this value represents the molar enthalpy for the formation of the catanionic surfactant, with a mean value of -388 ± 100 kJ mol^{-1}, at X_{SDS} roughly in the range 0.65−0.68, independent of the total concentration of both surfactants. The large error in the enthalpy is due to the fact that the concentration range of the peak is too small to measure exactly the location of the largest exothermic enthalpy in the automatic titration.

A more interesting feature is the appearance of two peaks following the formation of catanionic surfactant, in Figure 3b. According to the information from TEM, vesicle aggregates are imaged between points d and h. The insoluble catanionic surfactant starts redissolving at point d to form vesicle aggregates in coexistence with the solid, as indicated by the turbidity and TEM, until only vesicle aggregates are present at the top of the peak, e; thus, d−e is the third region. The transition enthalpy from catanionic surfactant to vesicle, ΔH_{CS-V}, is listed in Table 1; it can be that the corresponding X_{SDS} value decreases with the initial concentration of 12-6-12Br_2. The added SDS molecules incorporate into the vesicles to increase either the number of vesicles or the aggregation number of the vesicles, which corresponds to positive enthalpies (f−g). From point g, the vesicles transform into mixed micelles until point h, with the transition enthalpy, ΔH_{V-M}, and corresponding X_{SDS} also decreasing with the initial concentration of 12-6-12Br_2 (Table 1). The region between j and k most probably represents a transition between different micellar morphologies, but this is yet unclear. This region increases in width with the concentration of 12-6-12Br_2. Note that in Figure 4 the dilution isotherm of SDS is not shown, because the small dilution enthalpy does not affect evidently the interaction between both the surfactants; also, we only discuss the change of the observed enthalpies but not their absolute values, as done in other works.[21]

According to the discussion above, and upon comparison with TEM observations, the phase boundaries can be determined with good accuracy by the ITC isotherm, with an estimated error in X_{SDS} of ± 0.012. Therefore, the interaction enthalpies and phase transition enthalpies can be obtained from the observed enthalpy as shown in Figure 4b; those values are listed in Table 1. The interaction enthalpies are much larger than the enthalpies for

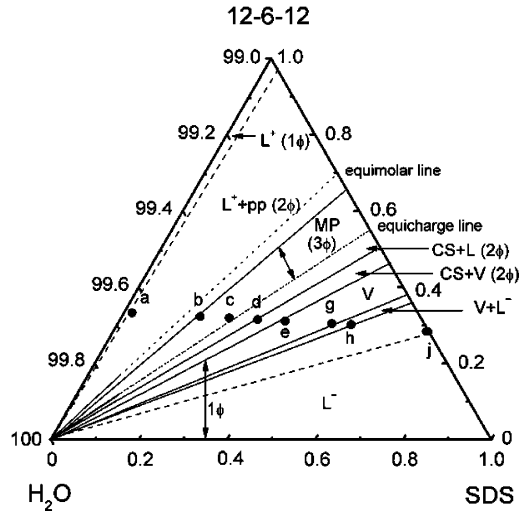

Figure 4. Triangular phase diagram for the catanionic mixture 12-6-12Br_2/SDS/water at the water-rich corner, at 30 °C, with indication of the aggregation structures as obtained from TEM and ITC methods. The letters a−j correspond to the location of the same samples as in Figure 3. Labels are as follows: L^+, gemini-rich micellar solution; pp, precipitate; MP, multiphase region (three-phase); CS, catanionic surfactant; L, liquid phase; V, vesicle solution; L^-, SDS-rich micellar solution.

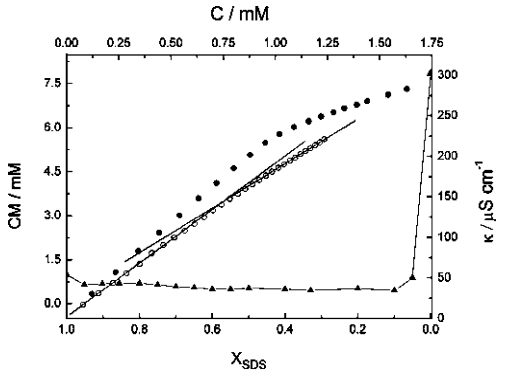

Figure 5. Plots of the conductivity for 12-6-12Br_2 (full circle) and for a representative mixture of 12-6-12Br_2 and SDS (empty circle), at $X_{SDS} = 0.80$, vs respective concentration (upper and right axis); also, the mixture cmc at 30 °C as a function of X_{SDS} (full triangle), with lower and left axis.

the catanionic surfactant−vesicle and vesicle−micelle transition, while the transition enthalpies for catanionic surfactant−vesicle are a little smaller than the ones from vesicle to micelle. The equal vesicle−micelle transition enthalpies at 5.0 mM and 3.5 mM of $C_{12-6-12}$ possibly indicate a similar micellar structure for both cases.

3.4. Global View of Phase Behavior and Aggregation in the 12-6-12Br_2/SDS/Water at the Water-Rich Corner. By combining the visual observations, turbidity measurements, TEM imaging, and ITC measurements, it is now possible to depict the phase behavior in a more detailed way. The observations are gathered in the triangular phase diagram shown in Figure 4, where the concentration of each component (12-6-12, SDS, and water) is given in weight percent with a maximum error of ±0.05. The lines for equimolar samples ($X_{SDS} = 0.50$) and for equicharged samples ($X_{SDS} = 0.66$) are drawn in the triangle as dashed lines.

The dashed line beside the binary axis of water and 12-6-12 indicates the phase boundary between the micellar solution (L^+) and the two-phase region solution + precipitate (L^+ + pp) with a relatively large uncertainty.

The three-phase region consisting of a bottom solid phase, a middle solution phase, and an upper phase (in small amount and, most likely, a liquid crystal) appears between the L^+ + pp and the CS + L two-phase regions. Here, L designates a very dilute aqueous solution (almost pure water, due to the low solubility of the catanionic solid). The boundary between this three-phase region and CS + L practically overlaps the equicharged line. By visual observation, it is difficult to distinguish between regions of CS + L and CS + V (catanionic surfactant + vesicles), but one can identify vesicle aggregates with TEM and determine the phase boundary with ITC. Beyond region CS + V, the one-phase region with vesicles (V) appears. The samples gradually show a lower amount of precipitate as the molar fraction of SDS departs from equal charge and the liquid phase changes from turbid to bluish without precipitate and a clear bluish phase, until a transparent colorless liquid is formed. There is a narrow region of vesicle and micelle coexistence (V + L^-), which appears as a single macroscopic phase. Inside the region L^-, a boundary can be drawn from the ITC isotherm, suggesting a transition between different micellar shapes, but which cannot be unequivocally verified by the methods used in this work. So, with ITC, not only the phase boundaries but also the transition region between two phases are confirmed. It should be stressed that the boundaries between the CS + V and V and between V + L^- and L^- regions change slightly with the total concentration of 12-6-12Br_2 and SDS, even though this is not evident enough to be seen in the triangle of Figure 4. From Table 1, it can be seen that the limiting value of X_{SDS} for the CS + V and V + L^- regions increases as $C_{12-6-12}$ decreases. This implies that the phase boundaries for these regions are not straight lines at the more dilute region of the phase diagram but slightly curved. Thus, for instance, upon dilution, a sample in the V + L^- region transforms into a V solution. The reason behind this lies in the cmc values of the mixture presented in Figure 5, which are around 1 mM in the SDS-rich side, as measured by conductivity. Upon dilution, when the mixture cmc is gradually approached, an increasing fraction of the total surfactant goes to the monomeric form. This fact has the consequence that the aggregate composition changes upon dilution, and the change may be significant enough for a change in aggregate structure or even in a macroscopic phase transition, as also observed in other catanionic systems.[9b]

3.5. Vesicle Formation and Stability. The formation of spontaneous vesicles by the catanionic 12-6-12Br_2/SDS mixture can, at first approach and in a simplistic way, be rationalized in terms of the geometric packing parameter model.[32,33] When the packing parameter, $v_{hc}/(a_o l_{hc})$, falls in the range 0.5−1, the surfactant tends to form bilayer aggregates with nonzero curvature. The packing parameter can also be seen as the ratio between the cross-section area of the chain and headgroup area, a_{hc}/a_o. The mixture of SDS with gemini reduces the electrostatic repulsions and hence reduces the mean area per headgroup, increasing the packing parameter. Hence, there will be a general trend for the mixture to form bilayer-based phases. We will analyze this in more detail.

First, it should be noticed that the vesicles in this system form for a bulk mixing molar ratio $2.9 < n_{SDS}/n_{gemini} < 3.8$, i.e., roughly when there are about 3−4 SDS molecules per gemini molecule, implying that there is a slight excess charge of the anionic surfactant. Since the hydrophobic moieties consist of identical alkyl chains for the two surfactants studied here, the areas occupied by the headgroups are the main factor to determine the packing parameter and hence the resulting aggregation. According to previous works,[35−39] the cross-section

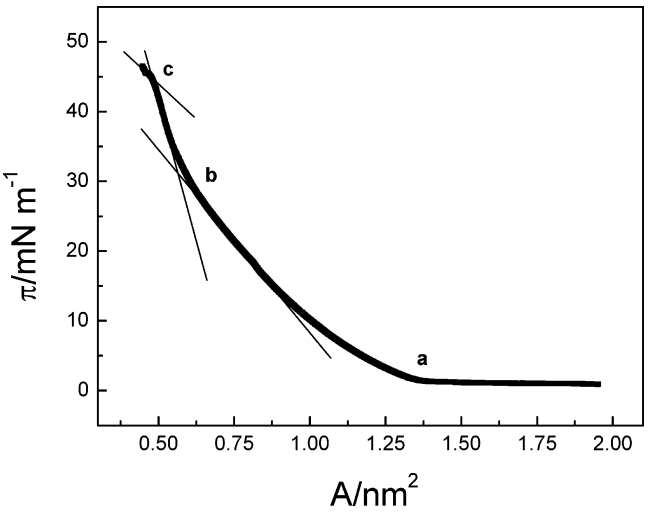

Figure 6. Surface pressure vs mean area per molecule for the mixture of 12-6-12Br_2 and SDS at $X_{SDS} = 0.66$ (equal charge) at 25 °C. Symbols a, b, and c correspond to the initial area for pressure rising, the phase transition between two liquid phases, and the collapse pressure, respectively.

area per fully extended alkyl chain is about 0.20 nm^2. In Figure 6, the surface pressure (π) − molecular area (A) isotherm obtained in this work for an equicharged mixture ($X_{SDS} = 0.66$) is shown, from which the packing parameter can be roughly evaluated. In Figure 6, a is the initial area for the surface pressure increase, b corresponds to a phase transition from liquid expanded phase to liquid condensed phase, and c is a collapse pressure (this and other results will be discussed in more detail in a forthcoming paper). The molecular organization at temperatures around room temperature has been considered a liquidlike morphology, in the discussion of spontaneous curvature.[40] The surface pressure of the solution at the saturated adsorption of the 12-6-12Br_2 and SDS mixture is situated in the liquid expanded phase (π is the difference between surface tension of pure water and that of the solution above cmc) in Figure 6. Accordingly, the mean area per molecule is about 0.6−0.9 nm^2 and the packing parameter on the order of 0.9−1.3 (>0.5), signifying that the molecular geometry should allow the formation of vesicle aggregates around the equicharged composition ($X_{SDS} = 0.66$).

In this system, the vesicles have been formed spontaneously, in the sense that no vigorous shearing forces produced by sonication, extrusion, and so forth have been used. These vesicles remain as a single-phase region for more than a year and are also found in long-term equilibrium with a solid and micelles (in the latter case, in a single macroscopic phase, similar to previously studied systems[9]). Such observations suggest that they can be thermodynamically stable. The equilibrium nature of vesicles formed in catanionic mixtures has been experimentally[9,10,34,41,42] and theoretically[42−46] discussed by several authors. The formation of a vesicle from a planar bilayer in a single-component system is thermodynamically unfavored due to the curvature energy penalty (frustration of one of the monolayers), despite the favorable entropic term (formation of many discrete aggregates from a single bilayer).[42,46] Two stabilization mechanisms can be considered in the mixture.[42] The curvature stabilization mechanism considers that spontaneous curvature of the bilayer may allow vesiculation due to the extra degree of freedom provided by composition asymmetry between the two monolayers, resulting from nonideal mixing due to the strong headgroup interactions. The mechanism can also involve oppositely charged surfactants of high asymmetry in chain lengths.[43] Such a mechanism would lead to small vesicles of narrow size distributions. The second mechanism involves an entropic stabilization in cases where the spontaneous curvature is not favorable but the bending penalty not too high (soft bilayers). This would lead to larger and more polydisperse vesicles. Bearing in mind this model, we can state that the bulk composition of the vesicle region, the imaged sizes (50−400 nm), and the results in Figure 6 suggest a possible mechanism for the stability of the SDS/12-6-12Br_2 vesicles. Different compositions in the inner and outer monolayers would allow for a curvature energy stabilization. The results from the $\pi-A$ isotherm show that an equicharged film adopts a negative spontaneous curvature, compatible with the curvature of the vesicle inner layer. The outer layer would then be enriched in SDS molecules and more charged, adopting the required positive spontaneous curvature. This picture is at this stage entirely hypothetical, as there is no available experimental evidence for the breakage of bilayer symmetry, except some indirect inferences from the data.

3.6. Comparison with Geminis with other Spacer Lengths. It should be noted that we also investigated, albeit to much lower extent, the phase behavior of SDS mixtures with 12-3-12Br_2 and with 12-10-12Br_2 (data not shown here). We also observed the aggregate morphologies in these two systems by TEM. The mixtures with 12-3-12Br_2 exhibit quite similar phase behavior to those of 12-6-12Br_2 and do not show any vesicles until X_{SDS} reaches 0.60, where interesting prolate-shaped vesicles with a mean diameter of about 100 nm and length of about 300 nm are observed. No vesicle aggregates have been found for the system with 12-10-12Br_2, which appears to be dominated by precipitate formation and spheroidal mixed micelles. As shown by Zana et al.,[6d] for 12-6-12Br_2 the spacer is of a length such that the distance between positive charges is comparable to that between separate molecules in an aggregate of the monomeric surfactant (DTAB). By comparison, vesicles are indeed spontaneously formed in the SDS-rich side of the SDS/DTAB system. If the spacer is shorter than 6, the packing parameter increases, and in the single gemini, this leads to the formation of wormlike or threadlike micelles. However, in the 12-3-12Br_2/SDS mixture, vesicles may still assemble, probably with a nonspheroidal shape, whereas for 12-10-12Br_2, the spacer seems to be too long and hydrophobic, favoring the solid and micelles rather than the vesicle shape.

4. Concluding Remarks

In this work, we have focused on the phase behavior and aggregate structure of the mixture of 12-6-12Br_2 and SDS. The results have shown that ITC is a good method to obtain the phase boundaries including the transition regions inside single phases by varying continuously the surfactant mixing ratio. Thus, interaction enthalpies between 12-6-12Br_2 and SDS, the transition enthalpies from catanionic surfactant to vesicle, and from vesicle to micelle, are available and can be used for further investigations of these systems. On the basis of turbidity, TEM, and ITC, it has been possible to build the phase diagram of this mixture at more than 99 wt % water. Both TEM and ITC allow us to identify a region of stable vesicle fromation in the SDS-rich side. A brief discussion of vesicle formation has been made on the basis of the simple packing parameter model, with a CPP value estimated from the measured $\pi-A$ isotherm.

Acknowledgment. We are grateful for financial support from the National Natural Science Foundation of China (grants no. 20073055 and 20173067). Y.W. is grateful to Fundação para a

Ciência e Tecnologia (F.C.T.), Portugal, for a post-doc grant, ref. SFRH/BPD/6979/2001. We kindly acknowledge finantial support from F.C.T., Portugal, and FEDER Funds, through the research project POCTI/QUI/44296/2002, and C.I.Q.(U.P.)-linha 5, F.C.T., Portugal.

References and Notes

(1) Menger, F. M.; Littau, C. A. *J. Am. Chem. Soc.* **1991**, *113*, 1451. (b) Menger, F. M.; Littau, C. A. *J. Am. Chem. Soc.* **1993**, *115*, 10083. (c) Menger F. M.; Mbadugha, B. N. A. *J. Am. Chem. Soc.* **2001**, *123*, 875.

(2) Zana, R. *Curr. Opin. Colloid Interface Sci.* **1996**, *1*, 556. (b) Zana, R. *Adv. Colloid Interface Sci.* **2002**, *97*, 205.

(3) Oda, R.; Huc, I.; Candau, S. J. *Angew. Chem., Int. Ed. Engl.* **1998**, *37*, 19, 2689. (b) Huc, I.; Oda, R. *Chem. Commun.* **1999**, 2025. (c) Oda, R.; Huc, I.; Danino, D.; Talmon, Y. *Langmuir* **2000**, *16*, 9759. (d) Knaebel, A.; Oda, R,; Mendes, E.; Candau, S. J. *Langmuir* **2000**, *16*, 2489.

(4) Rosen, M. J.; Mathias, J. H.; Davenport, L. *Langmuir* **1999**, *15*, 7340.

(5) Bai, G. Y.; Wang, J. B.; Yan, H. K.; Li, Z. X.; Thomas, R. K. *J. Phys. Chem. B* **2001**, *105*, 3105.

(6) Zana, R.; Talmon, Y. *Nature (London)* **1993**, *362*, 228. (b) Karaborni, S.; Esselink, K.; Hilbers, P. A. J.; Smit, B.; Karthäuser, J.; van Os, N. M.; Zana, R. *Science* **1994**, *266*, 254. (c) Danino, D.; Talmon, Y.; Levy, H.; Beinert, G.; Zana, R. *Science* **1995**, *269*, 1420. (d) Danino, D.; Talmon, Y.; Zana, R. *Langmuir* **1995**, *11*, 1448.

(7) Oda, R.; Huc, I.; Candau, S. J. *Chem. Commun.* **1997**, 2105.

(8) Menger, F. M.; Keiper, J. S.; Mbadugha, B. N. A. *Langmuir* **2000**, *16*, 9095.

(9) Khan, A.; Marques, E. F. *Curr. Opin. Colloid Interface Sci.* **2000**, *4*, 402. (b) Marques, E. F.; Regev, O.; Khan, A.; Miguel, M. G.; Lindman, B. *J. Phys. Chem. B* **1999**, *103*, 8353. (c) Marques, E. F.; Regev, O.; Khan, A.; Miguel, M. G.; Lindman, B. *J. Phys. Chem. B* **1998**, *102*, 6746. (d) Marques, E. F. *Langmuir* **2000**, *16*, 4798. (e) Marques, E.; Khan, A.; Miguel, M. G.; Lindman, B. *J. Phys. Chem.* **1993**, *97*, 4729.

(10) Kaler, E. W.; Herrington, K. L.; Murthy, A. K.; Zasadzinski, J. A. *J. Phys. Chem.* **1992**, *96*, 6698. (b) Herrington, K. L.; Kaler, E. W.; Miller, D. D.; Zasadzinski, J. A.; Chiruvolu, S. *J. Phys. Chem.* **1993**, *97*, 13792. (c) Brasher, L. L.; Herrington, K. L.; Kaler, E. W. *Langmuir* **1995**, *11*, 4267. (d) Brasher, L.; Kaler, E. *Langmuir* **1996**, *12*, 6270. (e) Yatcilla, M. T.; Herrington, K. L.; Brasher, L. L.; Kaler, E. W. *J. Phys. Chem.* **1996**, *100*, 5874.

(11) Bai, G. Y.; Wang, Y. J.; Wang, J. B.; Han, B. X.; Yan, H. K. *Langmuir* **2001**, *17*, 3522.

(12) Alargova, R. G.; Kochijashky, I. I.; Sierra, M. L.; Kwetkat, K.; Zana, R. *J. Colloid Interface Sci.* **2001**, *235* (1), 119.

(13) Bernheim-Groswasser, A.; Zana, R.; Talmon, Y. *J. Phys. Chem. B* **2000**, *104*, 12192.

(14) Bhattacharya, S.; De, S. *J. Chem. Soc., Chem. Commun.* **1995**, 651. (b) Bhattacharya, S.; De, S. *Langmuir* **1999**, *15*, 3400.

(15) Wang, Y. J.; Desbat, B.; Manet, S.; Aimé, C.; Labrot, T.; Oda, R. *J. Colloid Interface Sci.* **2005**, 283, 555.

(16) Oda, R.; Bourdieu, L. *J. Phys. Chem. B* **1997**, *101*, 5913.

(17) Zhao J.; Christian, S. D.; Fung, B. M. *J. Phys. Chem. B* **1998**, *102*, 7613.

(18) De, S.; Aswal, V. K.; Goyal, P. S.; Bhattacharya, S. *J. Phys. Chem. B* **1997**, *101*, 5639.

(19) Buwalda, R. T.; Engberts, J. B. F. N. *Langmuir* **2001**, *17* (4), 1054.

(20) Fukuda, H.; Kawata, K.; Okuda, H.; Regan, S. *J. Am. Chem. Soc.* **1990**, *112*, 1635.

(21) Meagher, R. J.; Hatton, T. A.; Bose, A. *Langmuir* **1998**, *14*, 4081. (b) Bai, G.; Wang, Y.; Wang, J.; Han, B.; Yan, H. *Langmuir* **2001**, *17*, 3522.

(22) Lukac, S.; Perovic, A. *J. Colloid Interface Sci.* **1985**, *103* (2), 586.

(23) Gucker, F. T., Jr.; Pickard, H. B.; Planck, R. W. *J. Am. Chem. Soc.* **1939**, *61*, 459.

(24) Wang, G.; Olofsson, G. *J. Phys. Chem.* **1995**, *99*, 5588.

(25) Jalzenjak, N.; Tezak, D. *Chem.—Eur. J.* **2004**, *10*, 5000.

(26) (a) Murray, R. C.; Hartley, G. S. *Trans. Faraday Soc.* **1935**, *31*, 183. (b) Murray, R. C. *Trans. Faraday Soc.* **1935**, *31*, 206.

(27) (a) Gharibi, H.; Palepu, R.; Bloor, D. M.; Hall, D. G.; Wyn-Jones, E. *Langmuir* **1992**, *8*, 782. (b) Palepu, R.; Gharibi, H.; Bloor, D. M.; Wyn-Jones, E. *Langmuir* **1993**, *9*, 110. (c) Charbit, G.; Dorion, F.; Gaboriaud, R. *J. Colloid Interface Sci.* **1985**, *106*, 265.

(28) Maeda, T.; Satake, I. *Bull. Chem. Soc. Jpn.* **1984**, *57*, 2386.

(29) Koshinuma, M. *Bull. Chem. Soc. Jpn.* **1981**, *54*, 3128.

(30) Brun, T. S.; Høiland, H.; Vikingstad, E. *J. Colloid Interface Sci.* **1978**, *63*, 590.

(31) Cutler, S. G.; Meares, P. *J. Chem. Soc., Faraday Trans. 1* **1978**, *74*, 1758.

(32) Tanford, C. *The Hydrophobic Effect*; Wiley: New York, 1980.

(33) (a) Israelachvili, N. J.; Mitchell, D. J.; Ninham, B. W. *J. Chem. Soc., Faraday Trans. 2* **1976**, *72*, 1525. (b) Israelachvili, N. J. *Intermolecular and Surface Forces*; Academic Press: New York, 1985.

(34) Kaler, E. W.; Herrington, K. L.; Murthy, A. K.; Zasadzinski, J. A. N. *J. Phys. Chem.* **1992**, *96*, 6698.

(35) (a) Viseu, M. I.; Gonçalves da Silva, A. M.; Costa, S. M. B. *Langmuir* **2001**, *17*, 1529−1537. (b) Gonçalves da Silva, A. M.; Viseu, M. I. *Colloids Surf., A* **1998**, *144*, 191.

(36) Dutta, P.; Peng, J. B.; Lin, B.; Ketterson, J. B.; Prakash, M.; Georgopoulos, P.; Ehrlich, S. *Phys. Rev. Lett.* **1987**, *58*, 2228.

(37) Evans, D. F.; Wennerström, H. *The Colloidal Domain: Where Physics, Chemistry, Biology, and Technology Meet*; VCH Publishers: New York, 1994; Chapter 2.

(38) Gaines, G. L., Jr. *Insoluble Monolayers at Liquid−Gas Interfaces*; Interscience: New York, 1966; Chapter 5.

(39) Zasadzinski, J. A.; Viswanathan, R.; Madsen, L.; Garnaes, J.; Schwartz, D. K. *Science* **1994**, *263*, 1726.

(40) (a) Helfrich, W. *Z. Natureforsch.* **1973**, *28c*, 693. (b) Helfrich, W. *Z. Natureforsch.* **1978**, *33a*, 305. (c) Helfrich, W.; Servuss, R. M. *Nuovo Cimento Soc. Ital. Fis, D* **1984**, *3*, 137.

(41) Hao, J. C.; Yuan, Z. W.; Liu, W. M.; Hoffmann, H, *J. Phys. Chem. B* **2004**, *108*, 5105.

(42) (a) Zemb, T.; Dubois, M. *Aust. J. Chem.* **2003**, *56*, 971. (b) Vautrin, C.; Dubois, M.; Zemb, T.; Schmölzer, S.; Hoffmann, H.; Gradzielski, M. *Colloids Surf., A* **2003**, *217*, 165. (c) Vautrin, C.; Zemb, T.; Schneider, M.; Tanaka, M. *J. Phys. Chem. B* **2004**, *108*, 7986.

(43) (a) Safran, S. A.; Pincus, P. A.; Andelman, D. A. *Science* **1990**, *248*, 354. (b) Safran, S. A.; Pincus, P. A.; Andelmann, D.; MacIntosh, F. C. *Phys. Rev. A* **1991**, *43*, 1071. (c) Safran, S. A.; MacKintosh, F. C.; Pincus, P. A.; Andelman, D. A. *Prog. Colloid Polym. Sci.* **1991**, *84*, 3.

(44) (a) Yuet, P. K.; Blankschtein, D. *Langmuir* **1996**, *12*, 3819. (b) Jung, H.-T.; Lee, S. Y.; Kaler, E. W.; Coldren, B.; Zasadzinski, J. A. *Proc. Natl. Acad. Sci. U.S.A.* **2002**, *99*, 15138.

(45) Laughlin, R. G. *Colloids Surf., A* **1997**, *128*, 27.

(46) Lasic, D. D.; Joannic, R.; Keller, B. C.; Fredrik, P. M. *Adv. Colloid Interface Sci.* **2001**, *89−90*, 337.